Field-induced tricritical behavior in the Néel-type skyrmion host GaV_4S_8

Bingjie Liu,[1,2] Zhe Wang,[1,3] Youming Zou,[1] Shiming Zhou,[4] Hexuan Li,[1,3] Jiemin Xu,[1,3] Lei Zhang,[1] Jingtao Xu,[5] Mingliang Tian,[1] Haifeng Du,[1] Yuheng Zhang,[1,4] and Zhe Qu[1,6,*]

[1]*Anhui Key Laboratory of Condensed Matter Physics at Extreme Conditions, High Magnetic Field Laboratory, Hefei Institutes of Physical Sciences, Chinese Academy of Sciences, Hefei, Anhui 230031, China*

[2]*School of Materials Science and Engineering, Beihang University, Beijing, 100191, China*

[3]*Science Island Branch of Graduate School, University of Science and Technology of China, Hefei, Anhui 230026, China*

[4]*Hefei National Laboratory for Physical Sciences at Microscale, University of Science and Technology of China, Hefei, Anhui 230026, China*

[5]*Ningbo Ruiling Advanced Energy Materials Institute Co., Ltd, Ningbo, Zhejiang 315500, China*

[6]*CAS Key Laboratory of Photovoltaic and Energy Conservation Materials, Hefei Institutes of Physical Sciences, Chinese Academy of Sciences, Hefei, Anhui 230031, China*

(Received 11 June 2020; revised 18 August 2020; accepted 8 September 2020; published 24 September 2020)

The lacunar spinel compound GaV_4S_8 exhibits a Néel-type skyrmion, which holds great promise for future spintronics and ultrahigh-density magnetic memory devices. To gain more insight into the magnetic interactions, the critical behavior of GaV_4S_8 is studied by dc magnetization measurement around the Curie temperature (T_C). A set of reliable critical exponents ($\beta = 0.220 \pm 0.024$, $\gamma = 0.909 \pm 0.005$, and $\delta = 5.161 \pm 0.003$) is obtained by the modified Arrott plot technique, the Kouvel-Fisher method, and critical isothermal analysis. The generated critical exponents fulfill the universality class of tricritical mean-field theory, which suggests a field-induced tricritical phenomenon. Based on the scaling equations, boundaries between the skyrmion and ferromagnetic phases can be distinguished. A tricritical point is revealed at the temperature of $T_{Tr} = 12$ K and field of $H_{Tr} = 60$ mT, which is located at the intersection point among the skyrmion, ferromagnetic, and paramagnetic phases. It is suggested that the origin of the tricritical behavior in GaV_4S_8 is related to the skyrmion state near the magnetic transition temperature T_C.

DOI: 10.1103/PhysRevB.102.094431

I. INTRODUCTION

The skyrmion state, a topologically protected nanoscale vortexlike spin structure, has attracted significant attention due to its potential application in high-density information storage technology [1–3]. For skyrmion configurations, there are two basic types classified by the magnetic domain walls [4,5]. One is the Bloch-type domain walls, where the spins rotate in the plane parallel to the domain boundary to form whirlpool-like skyrmions. Such Bloch vortices have been observed in chiral magnets, such as FeGe, MnSi, and Cu_2OSeO_3, etc. [1,3,6–9]. The other is the Néel-type domain walls with spins rotating in a plane perpendicular to the domain boundary, where the spins rotate in the radial planes from their cores to peripheries. The Néel-type domain walls are expected to emerge in polar magnets with C_{nv} crystal symmetry [4]. The polar magnetic semiconductor GaV_4S_8 has been reported as one of the rare materials which host the Néel-type skyrmion lattice. At room temperature, the crystal structure of GaV_4S_8 is a noncentrosymmetric cubic cell with space group $F\bar{4}3m$ [10]. It undergoes a cubic-to-rhombohedral structural phase transition at temperature $T_{JT} = 44$ K [11]. The magnetic order emerges below $T_C = 12.7$ K [11–14], which is slightly affected by the external field [15]. The weakly coupled cubane $(V_4S_4)^{5+}$ units form face-centered cubic lattices and are separated by a $(GaS_4)^{5-}$ tetrahedron. GaV_4S_8 exhibits various ordering phases, including ferromagnetic, cycloidal, and Néel-type skyrmion lattice phases. In particular, the skyrmion phase emerges in a narrow temperature range just below T_C and in the field range from 10 to 100 mT [4].

Recently, a field-induced tricritical phenomenon was revealed in the Bloch-type skyrmion materials, such as MnSi and Cu_2OSeO_3, which usually appears when the first-order transition is suppressed [16–18]. However, the critical behavior of the Néel-type skyrmion material has not been thoroughly investigated. In particular, multiple field-induced phases and tricriticality are expected in this system. Based on this motivation, critical behavior of the Néel-type skyrmion host GaV_4S_8 is investigated by means of bulk dc magnetization, which reveals a field-induced tricritical behavior. Moreover, a tricritical point is found to be located at the intersection point of the skyrmion, ferromagnetic, and paramagnetic phases.

II. EXPERIMENTAL METHODS

Polycrystalline GaV_4S_8 was prepared by solid-state reaction using high-purity Ga, V, and S in an appropriate ratio [14]. The structure was checked by powder x-ray diffraction (XRD). The XRD pattern was fitted by the Rietveld method,

*Corresponding author: zhequ@hmfl.ac.cn

which indicates a single phase. The magnetization of the sample was measured using a Quantum Design superconducting quantum interference device vibrating sample magnetometer (SQUID VSM). Isothermal magnetization was collected at an interval of 0.05 K around the Curie temperature. The no-overshoot mode was applied to ensure a precise magnetic field. In order to minimize the demagnetizing field, the sample was processed into a slender ellipsoid shape, and the magnetic field was applied along the longest axis [16]. The sample was first heated above T_C and then cooled to the target temperature before measurement to make sure each curve was initially magnetized. Moreover, the applied magnetic field H_a has been corrected into the internal field as $H = H_a – NM$ (where M is the measured magnetization and N is the demagnetization factor) [19]. The calculated H was used for the analysis of the critical behavior.

III. RESULTS AND DISCUSSION

Figure 1(a) depicts the temperature dependence of magnetization [$M(T)$] under an applied field of 1000 Oe with a zero-field cooling model. As shown in the inset of Fig. 1(a), a paramagnetic-to-ferromagnetic (PM-FM) transition occurs at $T_C = 12\,\text{K}$ determined by the tip on the curve of dM/dT vs T. Figure 1(b) gives the isothermal magnetization [$M(H)$] at $T = 2\,\text{K}$. The inset of Fig. 1(b) plots the magnified $M(H)$ in the low-field region, which shows that the saturation field $H_S \approx 10\,\text{kOe}$. Almost no magnetic hysteresis is found on the $M(H)$ curve, suggesting no coercive force in GaV_4S_8.

According to the theory of magnetic phase transition, one can characterize the critical behavior of a second-order phase transition using a series of critical exponents, β, γ, δ, etc., which are combined by magnetic equations of state [20,21]. The exponents β and γ can be obtained from spontaneous magnetization M_S and initial susceptibility χ_0 below and above T_C, respectively, while δ is the critical isotherm exponent. The mathematical definitions of the critical exponents are given as

$$M_S(T) = M_0(-\varepsilon)^{\beta}, \quad \varepsilon < 0, \quad T < T_C, \tag{1}$$

$$\chi_0^{-1}(T) = (h_0/M_0)\varepsilon^{\gamma}, \quad \varepsilon > 0, \quad T > T_C, \tag{2}$$

$$M = DH^{1/\delta}, \quad \varepsilon = 0, \quad T = T_C, \tag{3}$$

where $\varepsilon = (T - T_C)/T_C$ is the reduced temperature, and M_0, h_0/M_0, and D are the critical amplitudes. Moreover, the magnetic equation of state in the critical region can be described using the scaling functions,

$$M(H, \varepsilon) = \varepsilon^{\beta} f_{\pm}(H/\varepsilon^{\beta+\gamma}), \tag{4}$$

where f_+ for $T > T_C$ and f_- for $T < T_C$, respectively, are regular functions. Furthermore, the mathematical correlations for renormalized magnetization $m = \varepsilon^{-\beta}M(H, \varepsilon)$ and renormalized field $h = \varepsilon^{-(\beta+\gamma)}H$ fulfill

$$m^2 = f_{\pm}(h/m). \tag{5}$$

In this scenario, critical exponents are included in the critical region by using Eqs. (4) and (5), respectively.

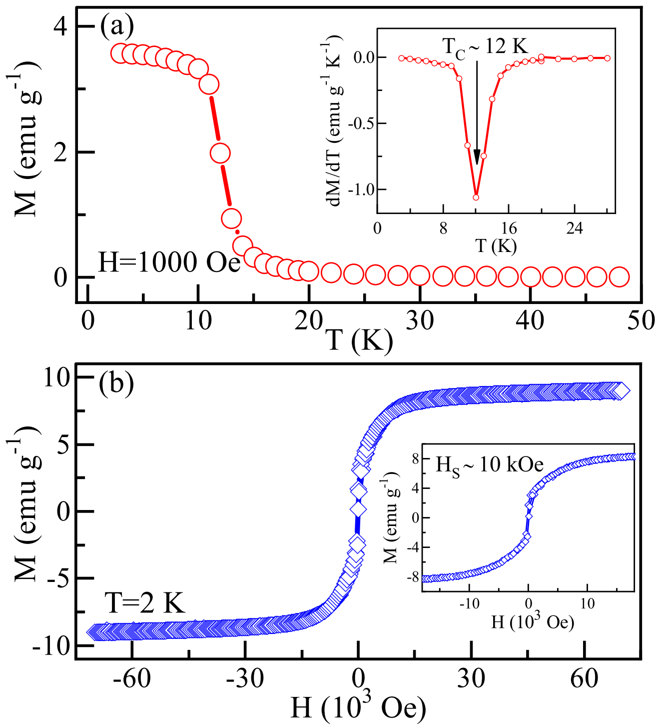

FIG. 1. (a) Temperature dependence of zero-field-cooling magnetization [$M(T)$] under $H = 1000\,\text{Oe}$ for GaV_4S_8 (inset plots dM/dT vs T); (b) isothermal magnetization [$M(H)$] at $T = 2\,\text{K}$ [inset shows the $M(H)$ in the low-field region].

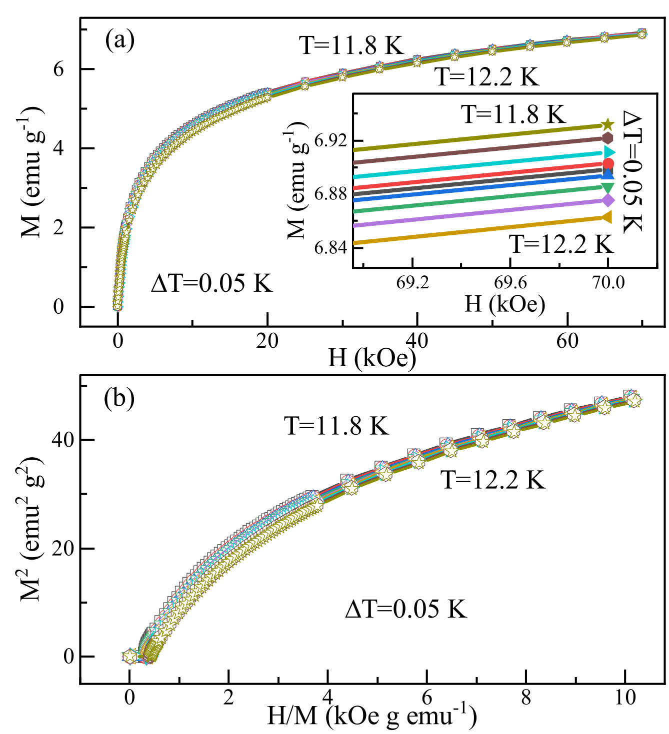

FIG. 2. (a) Isothermal magnetization curves in the vicinity of T_C [inset shows the enlarged view of $M(H)$ in the high-field region]; (b) Arrott plot (isotherms of M^2 vs H/M) for GaV_4S_8.

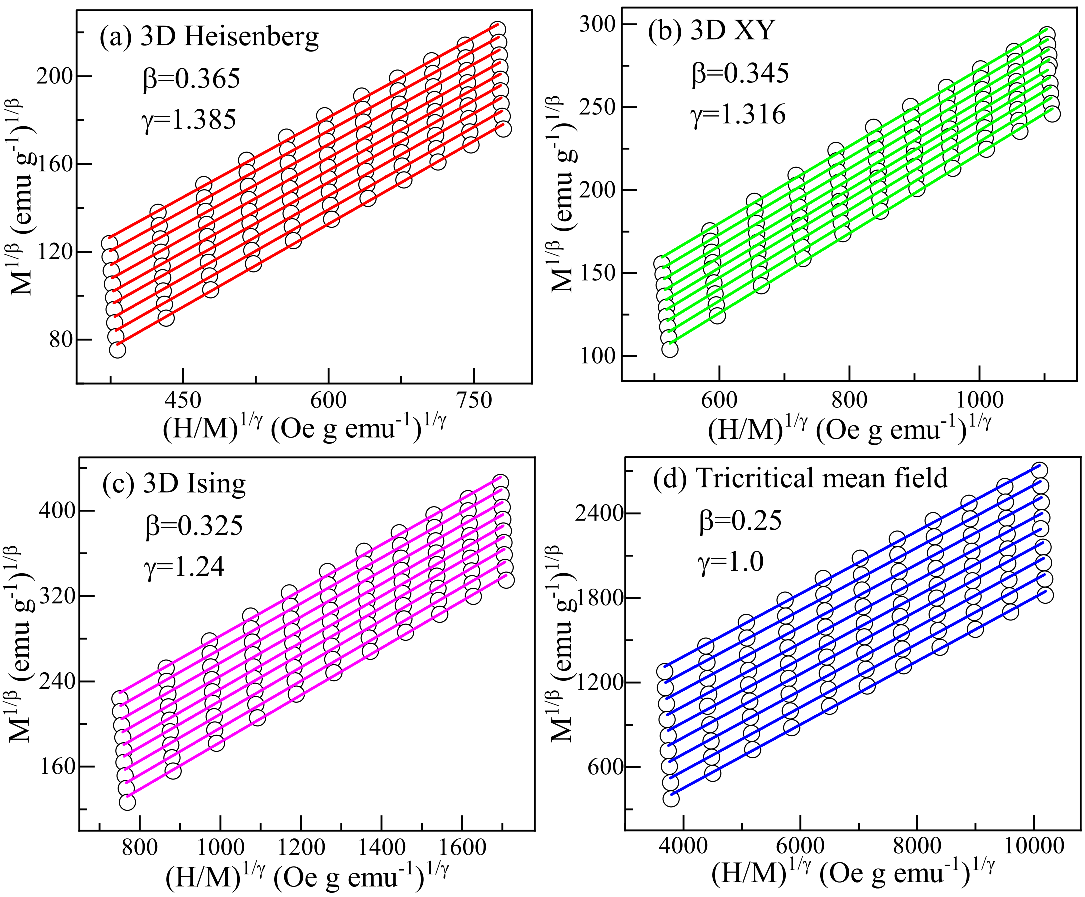

FIG. 3. Modified Arrott plot [isotherms of $M^{1/\beta}$ vs $(H/M)^{1/\gamma}$ with (a) 3D Heisenberg model ($\beta = 0.365,\ \gamma = 1.386$); (b) 3D XY model ($\beta = 0.345,\ \gamma = 1.316$); (c) 3D Ising model ($\beta = 0.325,\ \gamma = 1.24$); and (d) tricritical mean-field model ($\beta = 0.25,\ \gamma = 1.0$). Each curve was processed by a proper vertical translation for clear presentation.

In order to perform the critical phenomenon analysis, initial isothermal $M(H)$ curves within the critical region ($|\varepsilon| < 10^{-2}$) were collected as shown in Fig. 2(a). For the analysis of magnetic transition order in GaV_4S_8, we generate the Arrott plot of M^2 vs H/M in Fig. 2(b). According to Banerjee's criterion, the order of the magnetic transition can be judged by the slope of the high-field straight line: A positive slope corresponds to the second-order transition while the negative corresponds to the first-order one [22]. In this way, the positive slope in Fig. 2(b) indicates a second-order PM-FM transition in GaV_4S_8. Nevertheless, all curves in the Arrott plot are not rigorous straight lines even in the high-field region, suggesting the mean-field model with $\beta = 0.5$ and $\gamma = 1.0$ is not applicable to describe the critical phenomenon of GaV_4S_8.

Generally, the initial $M(H)$ curves around T_C should fulfill the Arrott-Noakes equation of state [23]:

$$(H/M)^{1/\gamma} = (T - T_C)/T_C + (M/M_1)^{1/\beta}, \tag{6}$$

where the $M^{1/\beta}$ vs $(H/M)^{1/\gamma}$ constitutes to the modified Arrott plot (MAP). In order to gain the critical exponents of GaV_4S_8, four kinds of theoretical models, including the three-dimensional (3D) Heisenberg model ($\beta = 0.365$, $\gamma = 1.386$), 3D XY model ($\beta = 0.345$, $\gamma = 1.316$), 3D Ising model ($\beta = 0.325$, $\gamma = 1.24$), and tricritical mean-field model ($\beta = 0.25$, $\gamma = 1.0$), are adopted to generate the MAPs [24,25]. As shown in Fig. 3, all MAPs based on the four models exhibit a bunch of quasistraight lines in the high-field region. In order to distinguish which model is the best, we extract the normalized slope $NS = S(T)/S(T_C)$ to compare them with the ideal value "1" [26]. As shown in Fig. 4, the normalized slope demonstrates that the tricritical mean-field model is the best interpretation for the critical behavior of GaV_4S_8.

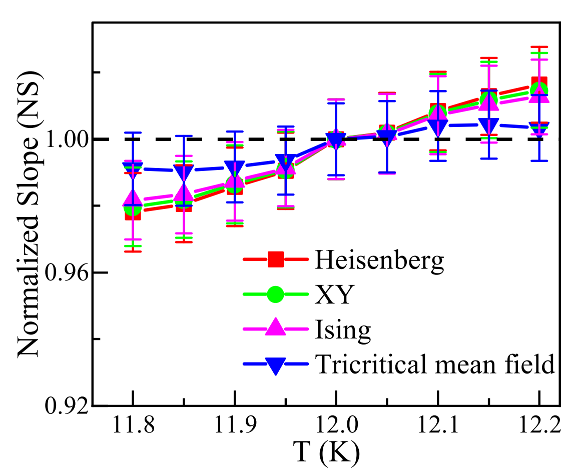

FIG. 4. Normalized slopes [$\mathrm{NS} = S(T)/S(T_C)$] of theoretical critical models as a function of temperature.

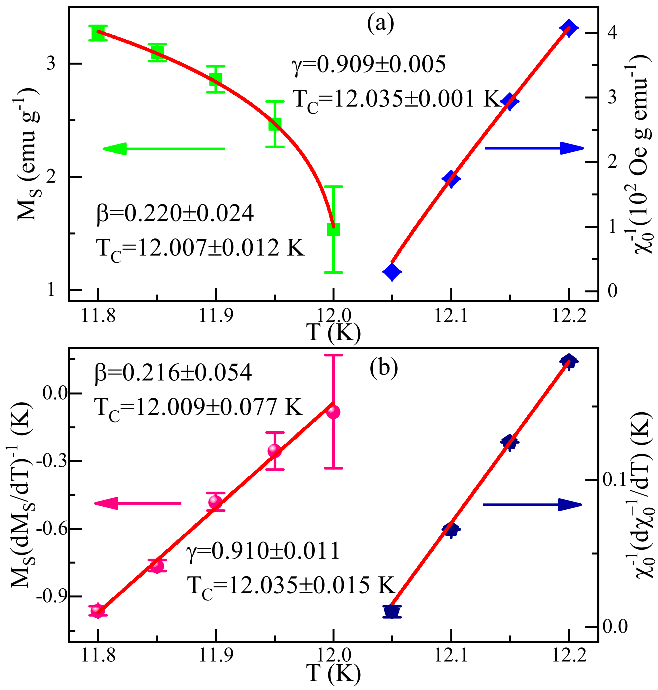

FIG. 5. (a) Temperature dependence of spontaneous magnetization M_S (left axis) and inverse initial susceptibility χ_0^{-1} (right axis) [the solid curves are fitted by Eqs. (1) and (2)]; (b) Kouvel-Fisher plot of M_S (left axis) and χ_0^{-1} (right axis) for GaV_4S_8 (straight lines are the linear fitting to the data).

In order to achieve the precise critical exponents β and γ, a rigorous iterative method is adopted [19]. The critical exponents of the tricritical mean-field model are chosen as the starting values. The starting values of $M_S(T)$ and $\chi_0^{-1}(T)$ are determined by the linear extrapolation from the high-field region to the intercepts with the axes $M^{1/\beta}$ and $(H/M)^{1/\gamma}$ in the former modified Arrott plot. New values of β and γ are obtained by following Eqs. (1) and (2), respectively. The critical temperature T_C is varied as a free parameter in the fitting process. This procedure is repeated until stable values of β, γ, and T_C are achieved. In this way, the finally obtained $M_S(T)$ and $\chi_0^{-1}(T)$ are plotted as a function of temperature in Fig. 5(a), which gives $\beta = 0.220 \pm 0.024$ with $T_C = 12.007 \pm 0.012$ and $\gamma = 0.909 \pm 0.005$ with $T_C = 12.035 \pm 0.001$ for GaV_4S_8. Moreover, the parameters $M_0 = 8.054 \pm 0.740$ and $h_0/M_0 = 20125.732 \pm 387.191$ are also obtained.

More accurately, the critical exponents can be obtained by the Kouvel-Fisher (KF) plot method [27]. According to the KF plot, the temperature dependence of $M_S(dM_S/dT)^{-1}$ and $\chi_0^{-1}(d\chi_0^{-1}/dT^{-1})$ should be straight lines with the slopes $1/\beta$ and $1/\gamma$, respectively. Meanwhile, the intercepts of the fitted straight lines on the temperature axis yield the critical temperature T_C. As shown in Fig. 5(b), from the fitted straight lines of $M_S(dM_S/dT)^{-1}$ and $\chi_0^{-1}(d\chi_0^{-1}/dT^{-1})$, it is obtained that $\beta = 0.216 \pm 0.054$ with $T_C = 12.009 \pm 0.077$ and $\gamma = 0.910 \pm 0.011$ with $T_C = 12.035 \pm 0.015$, respectively. Note that T_C's obtained from the modified Arrott plot and the KF plot show a very small difference with that deduced from $M(T)$ measurement and in other reports [4,15]. In fact, due

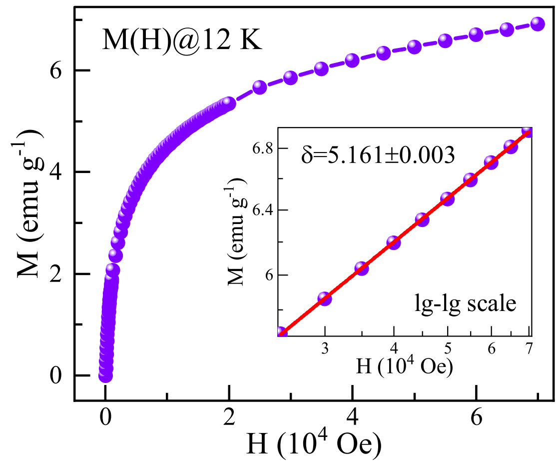

FIG. 6. Isothermal magnetization $[M(H)]$ at $T = 12\,\mathrm{K}$ for GaV_4S_8. The inset represents the same plot on a log-log scale with the fitted straight line following Eq. (3).

to the enhancement or weakening of the phase, the T_C can be changed by the external field. The fitting process in the modified Arrott plot and the KF method are extrapolated from a higher field, resulting in the slight difference. The critical exponents β, γ as well as T_C obtained by the modified Arrott plot and the KF plot match well enough, suggesting the results are reliable and unambiguous.

Figure 6 shows the isothermal magnetization $M(H)$ at $T = 12\,\mathrm{K}$ as well as its log-log plot in the inset. According to Eq. (3), the critical isotherm $M(H)$ at $T = T_C$ should behave as a straight line on log-log scale with the slope $1/\delta$. Consequently, a linear fitting to Eq. (3) in the inset of Fig. 6 yields the critical exponent $\delta = 5.161 \pm 0.003$. These critical exponents are unified by the Widom scaling law expressed as [28]

$$\delta = 1 + \frac{\gamma}{\beta}. \tag{7}$$

Using the independently obtained β and γ by modified Arrott plot and KF plot, $\delta = 5.132 \pm 0.109$ and $\delta = 5.213 \pm 0.250$, respectively, are yielded; the values are close to the experimentally obtained value (5.161 ± 0.003) generated from the critical isotherm. The results unambiguously indicate the self-consistency of the deduced critical exponents.

According to scaling theory, the $M(H)$ curves should collapse on two independent branches above and below the Curie temperature, respectively. Based on Eqs. (4) and (5), all data should follow two universal rules in the plots of $M|\varepsilon|^{-\beta}$ vs $H|\varepsilon|^{-(\gamma+\beta)}$ and m^2 vs h/m. As shown in Figs. 7(a) and 7(b), all experimental data in the high-field region collapse onto two independent branches: one for $T < T_C$ and the other for $T > T_C$. This scaling behavior clearly indicates that the magnetic interactions get properly renormalized following the scaling equations of state. Nevertheless, it is also noted that the low-field region below T_C cannot be collapsed onto one curve very well (shown in the insets of Fig. 7), which needs be investigated further. It has been indicated the of the uniaxial exchange anisotropy exits in single-crystal GaV_4S_8 by magnetization study [4]. It is shown that the strong anisotropy

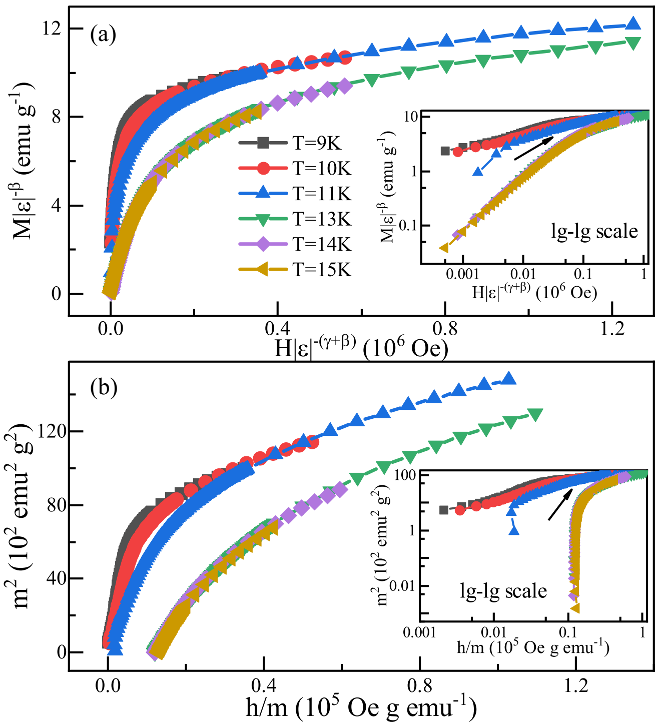

FIG. 7. (a) Scaling plots of renormalized magnetization m vs renormalized field h; (b) m^2 vs h/m around the critical temperature for GaV_4S_8. The insets are those on the log-log scale.

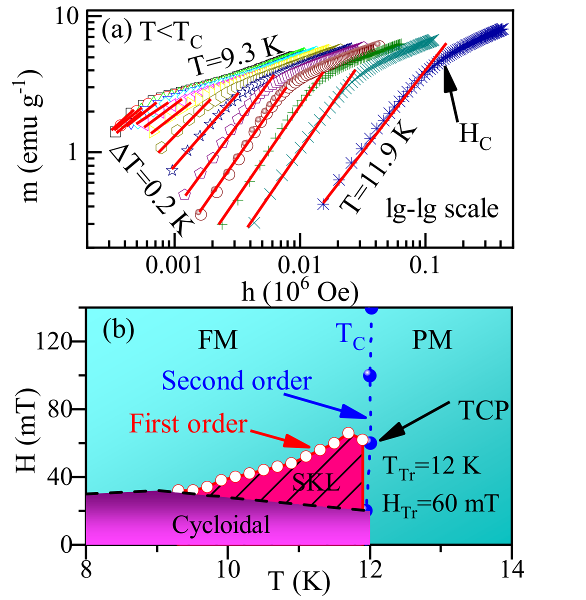

FIG. 8. (a) Magnified m vs h below T_C in the low-field region on a log-log scale with the fitted red solid lines; (b) the magnetic phase diagram of GaV_4S_8 derived from the $[M(T)]$ and critical analysis (SKL = skyrmion lattice). The cycloidal state is marked; refer to Ref. [4].

of GaV_4S_8 plays an important role in modulating low-field spin textures and skyrmion dynamics [15,29,30]. However, the sample used here is polycrystalline, in which anisotropy should not act very much.

In order to discover the low-field splitting of universality scaling phenomenon in Fig 7, we magnify the low-field isothermal magnetization curves of GaV_4S_8 with a temperature span from 9.3 to 11.9 K. The m vs h curves at low fields are shown in Fig. 8(a). It is clearly found that there is one turning point between low-field and higher-field data on each scaling curve. Moreover, the turning point changes monotonously with temperature. We extract those turning points on a magnetic phase diagram, as shown in Fig. 8(b). We note that, remarkably, all the turning points fall on the boundary between ferromagnetic and skyrmion lattice [4,13,30], which suggests that these turning points just distinguish the skyrmion and the ferromagnetic phases.

The critical exponents of GaV_4S_8 obtained from various methods, as well as those from different theoretical models and related skyrmion materials, are summarized in Table I for comparison. The critical exponents of GaV_4S_8 are very close to the tricritical mean-field model. It should be noted that the critical exponents of the Bloch-type skyrmion hosts FeGe and $Fe_{0.8}Co_{0.2}Si$ are close to the universality class of the 3D Heisenberg model, while MnSi is described with tricritical mean-field theory. In MnSi, a first-order phase transition induced by fluctuation is exhibited, which can be suppressed by field or pressure. When the first-order transition is suppressed, a tricritical mean-field behavior appears [16]. For Cu_2OSeO_3, its critical behavior approaches the 3D Heisenberg model under zero or very low field. However, recent investigation shows a field-induced tricritical phenomenon, where a tricritical point and a Lifshitz point are revealed [18]. The critical analysis of Cu_2OSeO_3 demonstrates that the critical behaviors and multiple phases can be modulated by external means.

As mentioned above, the critical exponent values of GaV_4S_8 are mostly close to those predicted by the tricritical mean-field theory, which unambiguously indicates a tricritical behavior. As is known, the tricritical phenomenon usually occurs at the boundary between a first-order phase transition and a second-order one, suggesting the rich variety in the phase diagram for GaV_4S_8. It should be pointed out that first-order phase transition from skyrmion to ferromagnetic here is judged only by the scaling analysis. Actually, the first-order nature of skyrmion-ferromagnetic and cycloidal-skyrmion phase transitions by small-angle neutron scattering (SANS) investigations of GaV_4S_8 has been indicated [4], which further confirms the reliability of the analysis of critical phenomena.

The existence of first-order transition in other lacunar spinel compounds should be noted. Another close V_4-cluster compound GeV_4S_8 undergoes an orbital and ferroelectric ordering at the Jahn-Teller transition around 30 K and exhibits antiferromagnetic order below about 14 K [33–35]. Moreover, the nature of both phase transitions in GeV_4S_8 is first order [35]. Therefore, it is suggested that the first-order characteristics in GaV_4S_8 might correlate with the lattice modulation from GeV_4S_8 to GaV_4S_8.

Furthermore, it is necessary to reveal the nature as well as the exchange distance in this material. As is known, for a homogeneous magnet, the universality class of the magnetic phase transition depends on the exchange distance $J(r)$. Considering that the interaction between spins is treated as an attractive interaction, a renormalization group theory analysis

TABLE I. Comparison of critical exponents determined from different methods of GaV_4S_8 with different theoretical models and related materials (MAP = modified Arrott plot; KFP = Kouvel-Fisher plot; PC = polycrystal; SC = single crystal; cal = calculated).

Composition	Reference	Technique	β	γ	δ
		MAP	0.220 ± 0.024	0.909 ± 0.005	5.132 ± 0.109^{cal}
$GaV_4S_8{}^{PC}$	This work	KFP	0.216 ± 0.054	0.910 ± 0.011	5.213 ± 0.250^{cal}
		Critical isotherm	–	–	5.161 ± 0.003
Mean field	[24]	Theory	0.5	1.0	3.0
3D Heisenberg	[24]	Theory	0.365	1.386	4.8
3D XY	[24]	Theory	0.345	1.316	4.81
3D Ising	[24]	Theory	0.325	1.24	4.82
Tricritical mean field	[25]	Theory	0.25	1.0	5
$MnSi^{SC}$	[16]	MAP	0.242 ± 0.006	0.915 ± 0.003	4.734 ± 0.006
$FeGe^{SC}$	[31]	MAP	0.336 ± 0.004	1.352 ± 0.003	5.267 ± 0.001
$Fe_{0.8}Co_{0.2}Si^{PC}$	[32]	Hall	0.371 ± 0.001	1.38 ± 0.002	4.78 ± 0.01
$Cu_2OSeO_3^{SC}$	[17]	AC	0.37(1)	1.44(4)	4.9(1)

suggests the interaction decays with distance r as [36,37]

$$J(r) \approx r^{-(d+\sigma)}, \tag{8}$$

where $d = 3$ is the spatial dimensionality and σ is a positive constant. Moreover, the susceptibility exponent γ is predicated as

$$\gamma = 1 + \frac{4}{d}\frac{n+2}{n+8}\Delta\sigma + \frac{8(n+2)(n-4)}{d^2(n+8)^2} \times \left[1 + \frac{2G\left(\frac{d}{2}\right)(7n+20)}{(n-4)(n+8)}\right]\Delta\sigma^2, \tag{9}$$

where $\Delta\sigma = (\sigma - \frac{d}{2})$ and $G(\frac{d}{2}) = 3 - (\frac{1}{4})(\frac{d}{2})^2$; n is the spin dimensionality. In this compound, it is found that $\sigma = 1.316 \pm 0.004$ from Eq. (9). Thus, the interaction distance decays as $J(r) \approx r^{-4.3}$.

IV. CONCLUSION

In summary, the critical behavior of the Néel-type skyrmion host GaV_4S_8 has been investigated around T_C. We obtain the reliable critical exponents ($\beta = 0.220 \pm 0.024$, $\gamma = 0.909 \pm 0.005$, and $\delta = 5.161 \pm 0.003$) by using various techniques including the modified Arrott plot technique, the Kouvel-Fisher method, and critical isotherm analysis. The critical exponents generated from different methods are self-consistent. The critical exponents of GaV_4S_8 belong to the universality class of the tricritical mean-field model, which unambiguously suggests a field-induced tricritical phenomenon. A tricritical point is determined as ($T_{Tr} = 12$ K, $H_{Tr} = 60$ mT), located at the intersection point among the skyrmion, ferromagnetic, and paramagnetic phases.

ACKNOWLEDGMENTS

This work was supported by National Natural Science Foundation of China (Grants No. U1832214, No. 11774352, No. 11874358, and No. 12074386).

[1] S. Muhlbauer, B. Binz, F. Jonietz, C. Pfleiderer, A. Rosch, A. Neubauer, R. Georgii, and P. Boni, Science **323**, 915 (2009).

[2] X. Z. Yu, Y. Onose, N. Kanazawa, J. H. Park, J. H. Han, Y. Matsui, N. Nagaosa, and Y. Tokura, Nature **465**, 901 (2010).

[3] S. Seki, X. Z. Yu, S. Ishiwata, and Y. Tokura, Science **336**, 198 (2012).

[4] I. Kézsmárki, S. Bordács, P. Milde, E. Neuber, L. M. Eng, J. S. White, H. M. Ronnow, C. D. Dewhurst, M. Mochizuki, K. Yanai, H. Nakamura, D. Ehlers, V. Tsurkan, and A. Loidl, Nat. Mater. **14**, 1116 (2015).

[5] A. Bogdanov and A. Hubert, J. Magn. Magn. Mater. **138**, 255 (1994).

[6] X. Z. Yu, N. Kanazawa, Y. Onose, K. Kimoto, W. Z. Zhang, S. Ishiwata, Y. Matsui, and Y. Tokura, Nat. Mater. **10**, 106 (2011).

[7] M. Uchida, N. Nagaosa, J. P. He, Y. Kaneko, S. Iguchi, Y. Matsui, and Y. Tokura, Phys. Rev. B **77**, 184402 (2008).

[8] A. Neubauer, C. Pfleiderer, B. Binz, A. Rosch, R. Ritz, P. G. Niklowitz, and P. Böni, Phys. Rev. Lett. **102**, 186602 (2009).

[9] T. Adams, A. Chacon, M. Wagner, A. Bauer, G. Brandl, B. Pedersen, H. Berger, P. Lemmens, and C. Pfleiderer, Phys. Rev. Lett. **108**, 237204 (2012).

[10] R. Pocha, D. Johrendt, and R. Pottgen, Chem. Mater. **12**, 2882 (2000).

[11] C. S. Yadav, A. K. Nigam, and A. K. Rastogi, Phys. B (Amsterdam, Neth.) **403**, 1474 (2008).

[12] H. Müller, W. Kockelmann, and D. Johrendt, Chem. Mater. **18**, 2174 (2006).

[13] E. Ruff, S. Widmann, P. Lunkenheimer, V. Tsurkan, S. Bordács, I. Kézsmárki, and A. Loidl, Sci. Adv. **1**, e1500916 (2015).

[14] Y. Sahoo and A. K. Rastogi, J. Phys.: Condens. Matter **5**, 5953 (1993).

[15] S. Widmann, E. Ruff, A. Günther, H. A. Krug von Nidda, P. Lunkenheimer, V. Tsurkan, S. Bordács, I. Kézsmárki, and A. Loidl, Philos. Mag. **97**, 3428 (2017).
[16] L. Zhang, D. Menzel, C. M. Jin, H. F. Du, M. Ge, C. J. Zhang, L. Pi, M. L. Tian, and Y. H. Zhang, Phys. Rev. B **91**, 024403 (2015).
[17] I. Zivkovic, J. S. White, H. M. Ronnow, K. Prsa, and H. Berger, Phys. Rev. B **89**, 060401(R) (2014).
[18] H. C. Chauhan, B. Kumar, J. K. Tiwari, and S. Ghosh, Phys. Rev. B **100**, 165143 (2019).
[19] A. K. Pramanik and A. Banerjee, Phys. Rev. B **79**, 214426 (2009).
[20] M. E. Fisher, Rep. Prog. Phys. **30**, 615 (1967).
[21] H. E. Stanley, *Introduction to Phase Transitions and Critical Phenomena* (Oxford University Press, London, 1971).
[22] S. K. Banerjee, Phys. Lett. **12**, 16 (1964).
[23] A. Arrott and J. E. Noakes, Phys. Rev. Lett. **19**, 786 (1967).
[24] S. N. Kaul, J. Magn. Magn. Mater. **53**, 5 (1985).
[25] K. Huang, *Statistical Mechanics*, 2nd ed. (Wiley, New York, 1987).
[26] J. Y. Fan, L. S. Ling, B. Hong, L. Zhang, L. Pi, and Y. H. Zhang, Phys. Rev. B **81**, 144426 (2010).
[27] J. S. Kouvel and M. E. Fisher, Phys. Rev. **136**, A1626 (1964).
[28] L. P. Kadanoff, Phys. Phys. Fiz. **2**, 263 (1966).
[29] E. M. Clements, R. Das, G. Pokharel, M. H. Phan, A. D. Christianson, D. Mandrus, J. C. Prestigiacomo, M. S. Osofsky, and H. Srikanth, Phys. Rev. B **101**, 094425 (2020).
[30] D. Ehlers, I. Stasinopoulos, V. Tsurkan, H. A. Krug von Nidda, T. Fehér, A. Leonov, I. Kézsmárki, D. Grundler, and A. Loidl, Phys. Rev. B **94**, 014406 (2016).
[31] L. Zhang, H. Han, M. Ge, H. F. Du, C. M. Jin, W. S. Wei, J. Y. Fan, C. J. Zhang, L. Pi, and Y. H. Zhang, Sci. Rep. **6**, 22397 (2016).
[32] W. Jiang, X. Z. Zhou, and G. Williams, Phys. Rev. B **82**, 144424 (2010).
[33] H. Chudo, C. Michloka, H. Nakamura, and K. Yoshimura, Phys. B (Amsterdam, Neth.) **378–380**, 1150 (2006).
[34] D. Bichler, V. Zinth, D. Johrendt, O. Heyer, M. K. Forthaus, T. Lorenz, and M. M. Abd-Elmeguid, Phys. Rev. B **77**, 212102 (2008).
[35] S. Widmann, A. Günther, E. Ruff, V. Tsurkan, H.-A. Krug von Nidda, P. Lunkenheimer, and A. Loidl, Phys. Rev. B **94**, 214421 (2016).
[36] M. E. Fisher, S.-k. Ma, and B. G. Nickel, Phys. Rev. Lett. **29**, 917 (1972).
[37] K. Ghosh, C. J. Lobb, R. L. Greene, S. G. Karabashev, D. A. Shulyatev, A. A. Arsenov, and Y. Mukovskii, Phys. Rev. Lett. **81**, 4740 (1998).